Variable capacitors in meander-suspended superconducting microbridge technology for high frequency applications

M. Schicke[1], A. Navarrini[2], and K.-F. Schuster[1]

[1]IRAM, Institute de Radio Astronomie Millimetrique, 300 Rue de la Piscine, 38406 St Martin d'Hères, France
[2]Radio Astronomy Lab (RAL), University of California, 601 Campbell Hall, Berkeley CA 94720-3411, USA

Abstract— **Variable capacitors in the fF to pF capacitance range are very interesting for high frequency applications like variable filters, couplers, resonators, etc. Our recent development permits to use meander-like suspensions for electrostatically actuated microbridges in Niobium (Nb) technology (see Fig. 1). The surface mounted fabrication procedure allows for integration of these devices with the standard Nb tunnel diode fabrication process as used for radio astronomical heterodyne detectors and superconducting electronic circuitry. We present the fabrication procedure, first meander suspended devices with a low actuation voltage range, and two filter designs for 22 GHz tunable band pass filters.**

***Index Terms*—variable capacitors, Nb, microbridge, MEMS (MicroElectroMechanical Systems), tunable filters**

I. Introduction

The development of superconducting RF MEMS is motivated by the possibility of compact and reliable tuning elements with very low loss. In recent work we developed a fabrication technology for surface mounted Niobium MEMS, which is compatible with the low temperature (<150°C) fabrication procedure of Nb-Al/AlOx-Nb SIS tunnel diodes, used in heterodyne high frequency mixers operated at 4 K. This permits the planar integration of the filters and detectors. In a simple geometry of a first design (see Fig. 1), the suspension of 700nm thick bridge layers was very rigid and required high actuation voltage. Thinner bridge layers (200nm to 300nm) revealed a strong differential stress. Due to the stress-induced deformation the bridge layers obtained a undesirable rigidity (saddle-like structure, see inset of Fig. 1). Nevertheless a considerable height variation at bias voltages of less than 50 V could be achieved. The working principle of microbridges with a thin bridge layer has already been demonstrated for test capacitors with areas close to 100µm×100µm and an air gap of 5 µm. The capacity (some tens of fF) of these devices could be varied by more than 10% by applying a voltage of 45V [1]. In this paper we describe the successful solution of the remaining stress problem which allows us to reduce the actuation voltage to ~10 V.

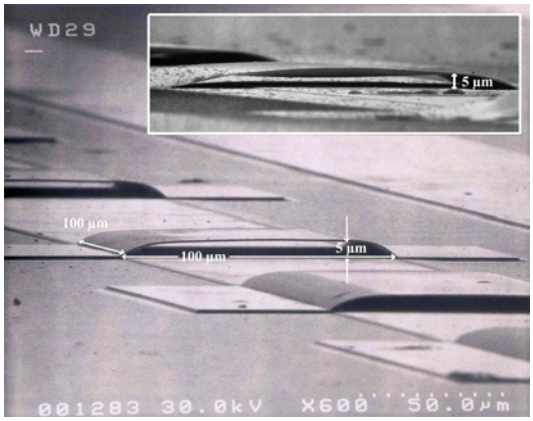

Figure 1: Example of a simple Nb thin film bridge. The Nb film of the bridge is 700 nm thick. The inset shows the extreme bending of a bridge layer with only 240nm thickness and the reduced height due to stress in the Nb film.

II. MEMS Fabrication Procedure

Most superconducting circuits and mm-wave detectors are based on superconducting Nb [2, 3]. Compared with galvanically grown bridge layers, sputtered Nb air bridges have the advantage, that the same techniques can be used as for the other parts of the superconducting circuitry.

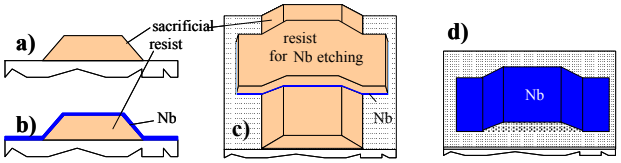

Figure 2: Fabrication process for sputtered Nb air bridges.

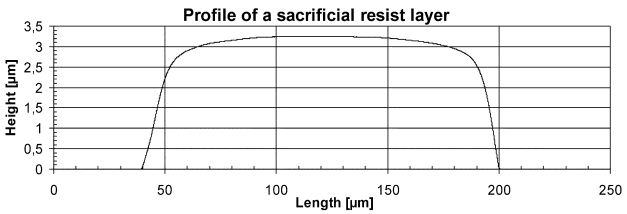

Figure 3: Profile of a sacrificial resist layer after flood exposure and development measured with a Dektak 8 profilometer.

After patterning of the attracting electrode using any suitable technique (e.g. lift-off or etching), a crucial step consists in the preparation of the sacrificial layer, which defines the bridge profile (Fig. 2a). Here, the photoresist AR-4000/8 (ALLRESIST) is used, giving an initial resist thickness of 5 µm. The pre-exposure bake is done for 30 minutes at 85°C in a convection oven. To obtain sufficiently smooth edges, the resist is baked 4 h at 94°C (flow bake) after development. Recent optimizations using proximity instead of contact exposure improved the edge smoothness and the total process time and hence replaced the flow bake. With an additional flood exposure the resist height can be adapted to a desired value. A resist profile can be seen in Fig. 3.

In the second step, the Nb layer is sputtered by DC-magnetron sputtering in periods of 5–10 s deposition and 5 min pause (Fig. 2b). Different step times have been chosen in order to examine a possible correlation with the film stress. The pauses are needed to reduce surface heating and thus deformation or polymerization of the resist layer.

The bridge widths and form of the suspensions are defined in the third step with a photo resist etch mask. For a good coverage of the structures, we use again the thick resist. Through this resist mask, which covers the surface of the Nb bridges, the non-covered parts of the Nb layer are etched by ICP (Inductively Coupled Plasma) etching, as shown in Fig. 2c [4].

In the final step, the resist is washed away in 70°C hot acetone (Fig. 2d).

Applying this new technique, bridges with Nb layers of 1.5 µm thickness were fabricated with lengths of 50–200 µm and widths of 50–1080 µm. A Nb film sputtered on top of the sacrificial resist layer prepared without flow bake shows a bending diameter of 1–2 mm. Taking a simple two-layer model one can estimate the compressive stress in the lower layer to be of the order of 100–200 MPa. This indicates that the film bending within the lengths of the bridges is much less pronounced than for 700 nm thick films with a bending diameter of 10–20 µm, corresponding to compressive stress of a few GPa. We tentatively explain this phenomenon with a strong stress gradient within the lower few hundred nm of the film thickness, whereas the upper part has almost no stress and serves therefore as stabilization. This effect can possibly be explained with the expansion and shrinking of the sacrificial resist layer during deposition and cooling, respectively, which might be more pronounced for the first hundreds of nm Nb thickness than for the last ones.

III. Meander-suspended Microbridges

Thin film structures from Niobium have great rigidity as can be seen from the Young's modulus of 105 GPa. This fact and the possibility to etch thick Nb layers highly anisotropically by ICP etching with helium substrate cooling opened the opportunity to introduce meander-like spring suspensions for variable capacities (see Fig. 4). With this type of suspension the spring constant can be adjusted through the meander dimensions.

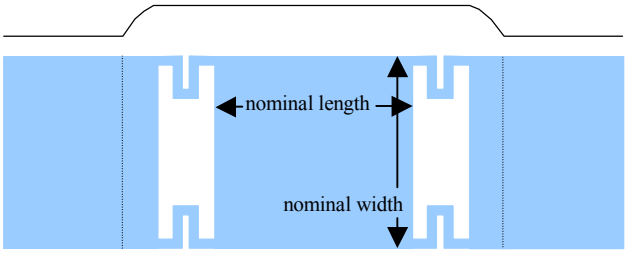

Figure 4: Schematic of a meander-suspended microbridge.

The fabrication of differently sized test bridges with differently sized meander suspensions showed that bridges with lengths of up to 100 µm and widths of up to 600 µm could be fabricated yielding more than 80% (see Fig. 5), whereas the bridges longer than 200 µm were often sticking on the ground after the washing of the sacrificial resist layer. With the actual recipe the bridge height can be chosen between 2 µm and 7 µm, but tests indicate that bridge heights down to 1 µm might be achievable.

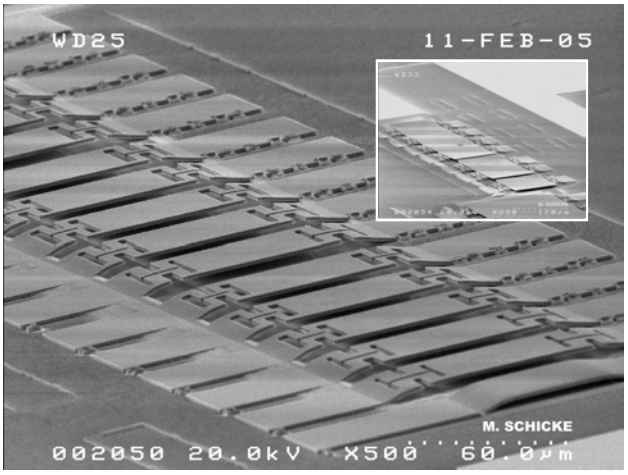

Figure 5: Series of 50µm-bridges with different meander dimensions. The bridge height is 3 µm and the Nb film thickness is 1.5 µm. In the inset a series of 100µm-bridges with widths from 180 µm to 600 µm can be seen.

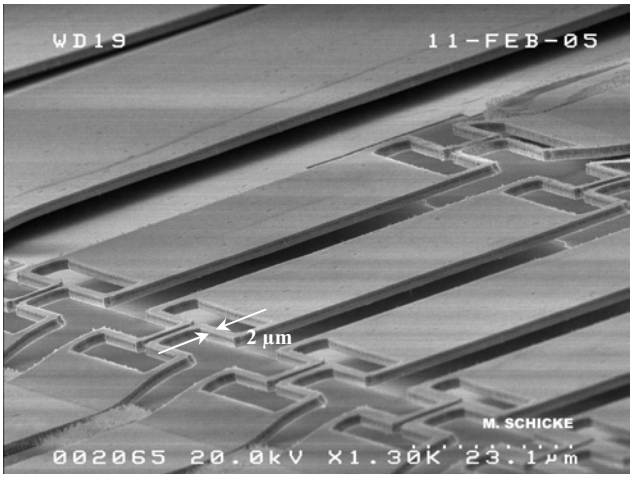

Figure 6: Series of 50µm-bridges with 2 µm wide meanders.

It has been demonstrated that even bridges with meander widths of 2 µm could be fabricated (see Fig. 6). Measurements of the capacitance were done with an Agilent LCR meter in a 4-point configuration. The variation of differently sized test bridges gave very promising results, as can be seen on Fig. 7. Only the 100x100 µm^2 bridges with meanders larger than 4 µm and shorter than 25 µm had their pull-in point above 40 V. From the capacitance value of the 150µm-bridge one can deduce an effective unbiased bridge height after release of 1 µm instead of 3 µm given by the thickness of the sacrificial resist layer. We explain this reduced height with the bending of the Nb bridge layer.

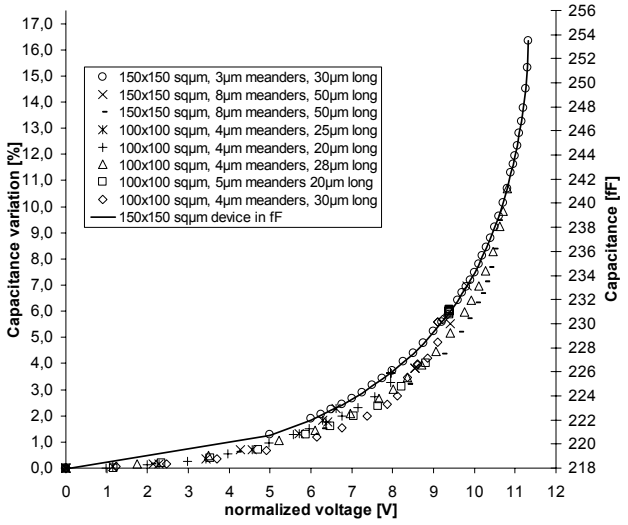

Figure 7: Capacitance of different meander-suspended microbridges as a function of the actuation voltage. The continuous line belongs to the right scale and the voltage scale shows the real voltages applied to this device. Points belong to various devices and capacity (left scale) has been normalized in order to show the similarity in actuation behavior.

IV. Band Pass Filters

The two filter chips, shown in Fig. 8, have been realized on quartz substrates with dimensions of 0.2×1.0×7.7 mm^3. Each of them has been synthesized starting from a lumped element model consisting of series inductors and parallel capacitors, which have been successively transformed in short sections (l<<λ) of, respectively coplanar waveguides (CPW) and microbridge lines. The electrodes underneath the bridges have almost the same size as the bridges. Both filters are optimized to provide maximum tuning frequency range when the air gaps of the microbridges are decreased from their nominal (unbiased) value of 2.5 µm down to the minimum of ~1.7 µm, expected when the maximum bias voltage is applied.

The filters were optimized using the commercial software ADS [5]. The microbridge structures and the effects of discontinuities between these sections and the CPW sections were modeled with Sonnet [6] and were successively included in ADS for global optimization of the filters. The superconducting effects, that slightly modify the transmission line properties due to the field penetration depth inside the 150 nm thick Nb layers, were taken into account in the electromagnetic simulations. The input and output sections of both filters are 50 Ω CPW with 260 µm wide central conductor

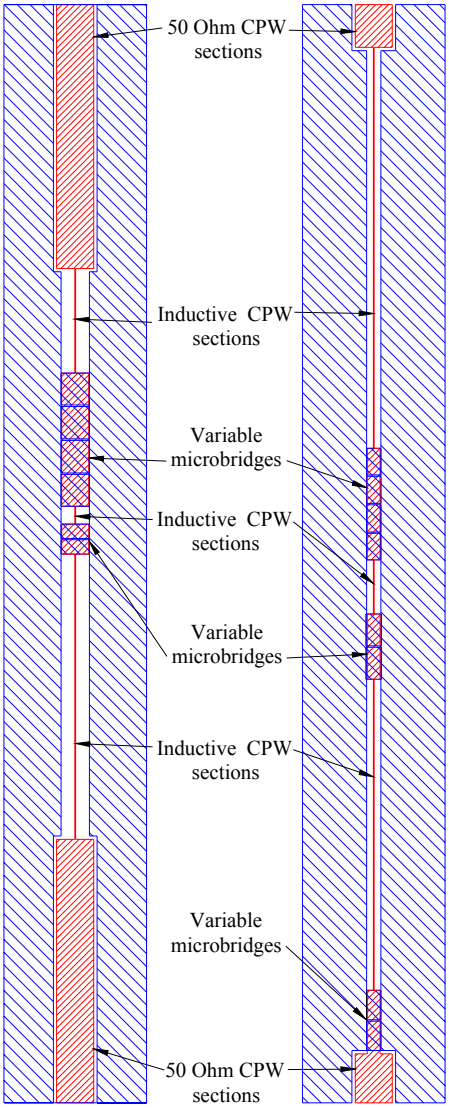

Figure 8: View of bandpass tunable filter chips: a) of order 5, b) of order 6.

and 23 µm gap to adjacent ground electrodes. The microbridges of each filter have all the same length (200 µm in the filter of order 5, 100 µm in the filter of order 6). The maximum width of the microbridges is 224 µm, and the narrowest central strip of the CPW sections is 5 µm. Because of the shorter microbridge length, the filter of order 6 can be realized with a higher yield than the other one, which has, nevertheless, the advantage that it can be tuned over a wider frequency range.

The results of the simulations for the transmitted amplitudes of the two filters under biased and unbiased conditions are shown in the Figs. 9 and 10. The central frequency of the filter can be tuned continuously within the respective range. The 3-dB fractional bandwidth of the filter is about 3% and varies only slightly with the voltage applied to the microbridges (between 670 MHz and 760 MHz). The estimated insertion losses are very low (< 0.3 dB), and vary little with bridge height. The off resonance isolation is below -17 dB.

First filter devices have been fabricated (Fig. 11) and are about to be measured.

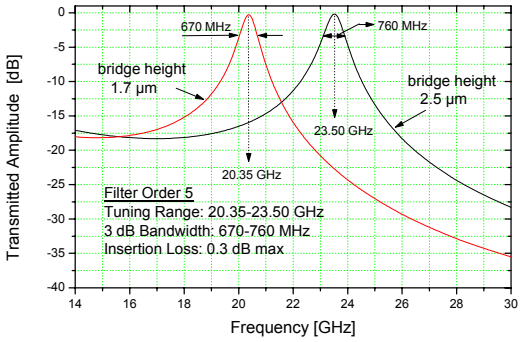

Figure 9: Transmitted amplitude of the filters of order 5 for two different air bridge heights: 2.5 µm (no voltage applied), and 1.7 µm (maximum voltage).

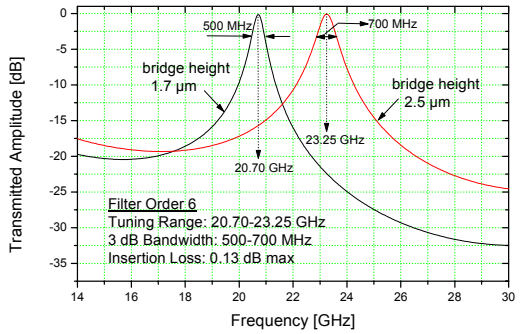

Figure 10: Transmitted amplitude of the filters of order 6 for two different air bridge heights: 2.5 µm (no voltage applied), and 1.7 µm (maximum voltage).

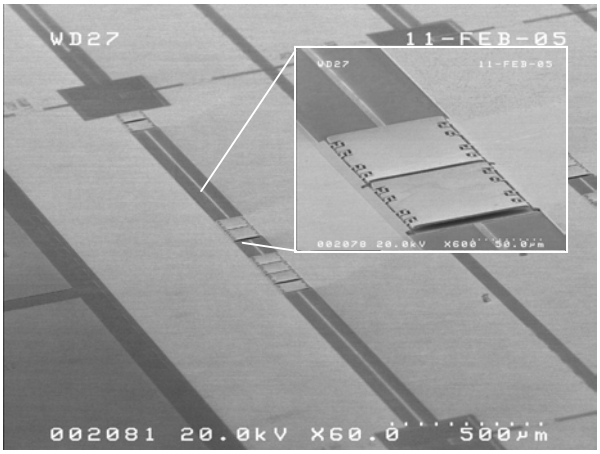

Figure 11: A 22 GHz band pass Filter device of order 6.

V. Outlook

One important aspect of variable microwave filter devices is the tunability band. The relative band of tunability is proportional to the relative variation ΔC/C of the micro-bridge's capacitance obtained by applying an actuation voltage or not. The value ΔC/C can be considerably increased by using a dielectric layer with high dielectric constant between the microbridge and the ground plane, as shown in Figure 12.

The capacitance C_{off} (no voltage applied) of two plane conductors separated by a distance h1+h2, where h1 is an air gap and h2 is a dielectric (AlN for example), is equivalent to a series of two capacitors C1 and C2 where C1 is the

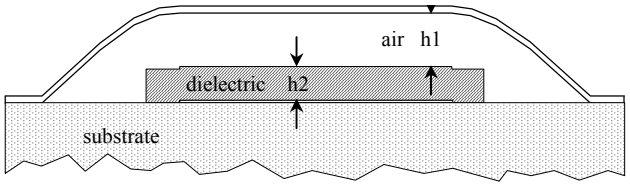

Figure 12: Schematic of a microbridge with additional dielectric layer.

capacitance of two conductors separated by a gap of air h1, and C2is the capacitance of two conductors separated by a h2 thick dielectric. The maximum relative variation of the capacitance is given by: $\Delta C/ C_{off} = (C2-C_{off})/C_{off} = \varepsilon_r\, h2/h1$. For example, if we use air only (with no dielectric) like in our 22 GHz filter design, with $\varepsilon_r=1$, h1=0.8 µm, h2=1.7 µm, we get: $\Delta C/ C_{off}=47\%$. If we add a dielectric layer of AlN (ε_r =4.6, [7]) with h2=1.7 um, and air h1=0.8 um, we obtain $\Delta C/C_{off}=216\%$.

Therefore, future improvements will include separation of actuation electrodes from tuned capacities. Topological variations of either top or ground electrodes can lead to much wider tuning ranges. Finally, dielectric layers will further improve tuning ranges and at the same time resolve problems of electrical isolation and sticking.

VI. Acknowledgements

The authors would like to thank A. Salvador Matar for his help in process optimization and T. Scherer for many helpful discussions. This project has been supported by ADIXEN-ALCATEL Vacuum Technology.

VII. References

[1] M. Schicke and K.F. Schuster, "Integrated Niobium Thin Film Air Bridges as Variable Capacitors for Superconducting GHz Electronic Circuits",*IEEE Trans. on Appl. Supercond.*, Houston, Texas, USA, June 2003.

[2] J. Zmuidzinas and P.L. Richards, "Superconducting Detectors and Mixers for Millimeter and Submillimeter Astrophysics", *Proceedings of the IEEE*, Vol. 92, No. 10, October 2004.

[3] K.H. Gundlach and M. Schicke, "SIS and bolometer mixers for terahertz frequencies", *Supercond. Sci. Technol.* 13 R171-R187, 2000.

[4] K.F. Schuster et al., "Inductively coupled plasma etching of Nb, NbN and Ta", 2005, submitted to Journal of Vacuum Science and Technology B.

[5] ADS (Advanced Design System), Agilent Technologies, http://eesof.tm.agilent.com/products/adsoview.html

[6] Sonnet Software, Inc., 1020 Seventh North Street, Suite 210, Liverpool, NY 13088, USA, http://www.sonnetsoftware.com

[7] Y. Goldberg, "Properties of advanced Semiconductor Materials GaN, AlN, InN, BN, SiC, SiGe", Eds. M.E. Levinshtein, S.L.Rumyantsev, M.S. Shur, John Wiley & Sons, Inc. New York, 2001, 31-47.